Role of Active Site Binding Interactions in 4-Chlorobenzoyl-Coenzyme A Dehalogenase Catalysis †

ARTICLE *in* BIOCHEMISTRY · JANUARY 2002

Impact Factor: 3.02 · DOI: 10.1021/bi011536f · Source: PubMed

6 AUTHORS, INCLUDING:

Lusong Luo
BeiGene
56 PUBLICATIONS **1,388** CITATIONS

SEE PROFILE

Role of Active Site Binding Interactions in 4-Chlorobenzoyl-Coenzyme A Dehalogenase Catalysis†

Lusong Luo, Kimberly L. Taylor, Hong Xiang, Yansheng Wei, Wenhai Zhang, and Debra Dunaway-Mariano*

Department of Chemistry, University of New Mexico, Albuquerque, New Mexico 87131

Received July 23, 2001; Revised Manuscript Received October 29, 2001

ABSTRACT: 4-Chlorobenzoyl-coenzyme A (4-CBA-CoA) dehalogenase catalyzes the hydrolytic dehalogenation of 4-CBA-CoA to 4-hydroxybenzoyl-CoA (4-HBA-CoA) via a multistep mechanism involving initial attack of Asp145 on C(4) of the substrate benzoyl ring to form a Meisenheimer intermediate (EMc), followed by expulsion of the chloride ion to form an arylated enzyme intermediate (EAr) and then ester hydrolysis in the EAr to form product. This study examines the role of binding interactions in dehalogenase catalysis. The enzyme and substrate groups positioned for favorable binding interaction were identified from the X-ray crystal structure of the enzyme−4-HBA-3′-dephospho-CoA complex. These groups were individually modified (via site-directed mutagenesis or chemical synthesis) for the purpose of disrupting the binding interaction. The changes in the Gibbs free energy of the enzyme−substrate complex ($\Delta\Delta G_{ES}$) and enzyme−transition state complex ($\Delta\Delta G^{\ddagger}$) brought about by the modification were measured. Cases where $\Delta\Delta G^{\ddagger}$ exceeds $\Delta\Delta G_{ES}$ are indicative of binding interactions used for catalysis. On the basis of this analysis, we show that the H-bond interactions between the Gly114 and Phe64 backbone amide NHs and the substrate benzoyl C═O group contribute an additional 3.1 kcal/mol of stabilization at the rate-limiting transition state. The binding interactions between the enzyme and the substrate CoA nucleotide moiety also intensify in the rate-limiting transition state, reducing the energy barrier to catalysis by an additional 3.3 kcal/mol. Together, these binding interactions contribute $\sim 10^6$ to the k_{cat}/K_m.

4-Chlorobenzoyl-coenzyme A (4-CBA-CoA)[1] dehalogenase catalyzes the central reaction of the 4-chlorobenzoate (4-CBA) to 4-hydroxybenzoate (4-HBA) pathway found in certain soil-dwelling bacteria (Scheme 1) (*4*). This pathway provides entry into the central oxidative aromatic pathways (*5*) and, thus, a way for the host bacterium to utilize 4-CBA as an alternate energy source.

The mechanism for 4-CBA-CoA dehalogenase catalysis is summarized in Figure 1 (*6*−*14*). Accordingly, substrate binding to the dehalogenase active site is followed by attack of the carboxylate side chain of Asp145 at benzoyl C(4). The Meisenheimer complex (EMc) thus formed expels chloride ion to produce the arylated enzyme intermediate (EAr). Hydrolysis of the ester function in the EAr then occurs to generate the 4-HBA-CoA product, which along with a proton and the chloride ion is released from the enzyme active site.

The X-ray crystal structure of the 4-CBA-CoA dehalogenase−4-HBA-3′-dephospho-CoA complex has been determined at 1.8 Å resolution (*15*).[2] Bound to the enzyme, the ligand assumes a hook-shaped conformation in which a tight turn at the pyrophosphate brings the ligand pantothenate and the pyrophosphate moieties out of one surface depression on the enzyme and into a second one (Figure 2). Thus, while the benzoyl and adenosine portions of the ligand are buried within the two crevices, the pantothenate and the pyrophosphate moieties are partially solvent exposed.

The potentially favorable interactions between the enzyme and product ligand that are evident from the X-ray crystal structure are illustrated in Figure 3. The 4-hydroxyl group of the benzoyl ring H-bonds with the carboxylate group of Asp145, while the benzoyl ring itself is surrounded by the aromatic rings of Phe64, Phe82, Trp89, and Trp137. The benzoyl C═O group is positioned for H-bonding to the backbone amide NHs of Phe64 and Gly114 and for electrostatic interaction with the positive pole of the 114−125 α-helix. The phosphoryl groups of the CoA unit form ion pairs with the charged side chains of Arg24, Arg257, and Arg67, while the adenine C(6)NH_2 group engages in H-bond interaction with the backbone C═O group of Phe64. Note that the backbone amide NH group of this same residue

† This research was supported by NIH Grant GM28688 to D.D.-M.

* To whom correspondence should be addressed. Phone: (505) 277-3383. Fax: (505) 277-6202. E-mail: dd39@unm.edu.

[1] Abbreviations: EMc, Meisenheimer intermediate; EAr, arylated enzyme intermediate; ES, enzyme−substrate complex; EP, enzyme−product complex; 4-CBA, 4-chlorobenzoate; 4-HBA, 4-hydroxybenzoate; CoA, coenzyme A; 4-CBA-CoA, 4-chlorobenzoyl-coenzyme A; 4-HBA-CoA, 4-hydroxybenzoyl-coenzyme A; 4-MeBA-CoA, 4-methylbenzoyl-coenzyme A; 4-CBA-dithio-CoA, 4-chlorobenzoyldithio-coenzyme A; 4-HBA-dithio-CoA, 4-hydroxybenzoyldithio-coenzyme A; ϵ-CoA, 1,N^6-ethenocoenzyme A; 3′,5′-ADP, adenosine 3′,5′-diphosphate; 3′-P,5′-ADP, adenosine 3′-phospho-5′-diphosphate; 5′-AMP, adenosine 5′-monophosphate; 5′-ADP, adenosine 5′-diphosphate; ATP, adenosine 5′-triphosphate; PP_i, inorganic pyrophosphate; NMR, nuclear magnetic resonance; WT, wild-type; DTT, dithiothreitol; Hepes, *N*-(2-hydroxyethyl)piperzine-*N*′-2-ethanesulfonic acid; HPLC, high-performance liquid chromatography.

[2] The dehalogenase was cocrystallized with synthetic 4-HBA-CoA which contains 4-HBA-3′-phospho-CoA as a contaminant. The crystals formed from the enzyme bound with this contaminant.

10.1021/bi011536f CCC: $22.00
Published on Web 00/00/0000 PAGE EST: 8.5

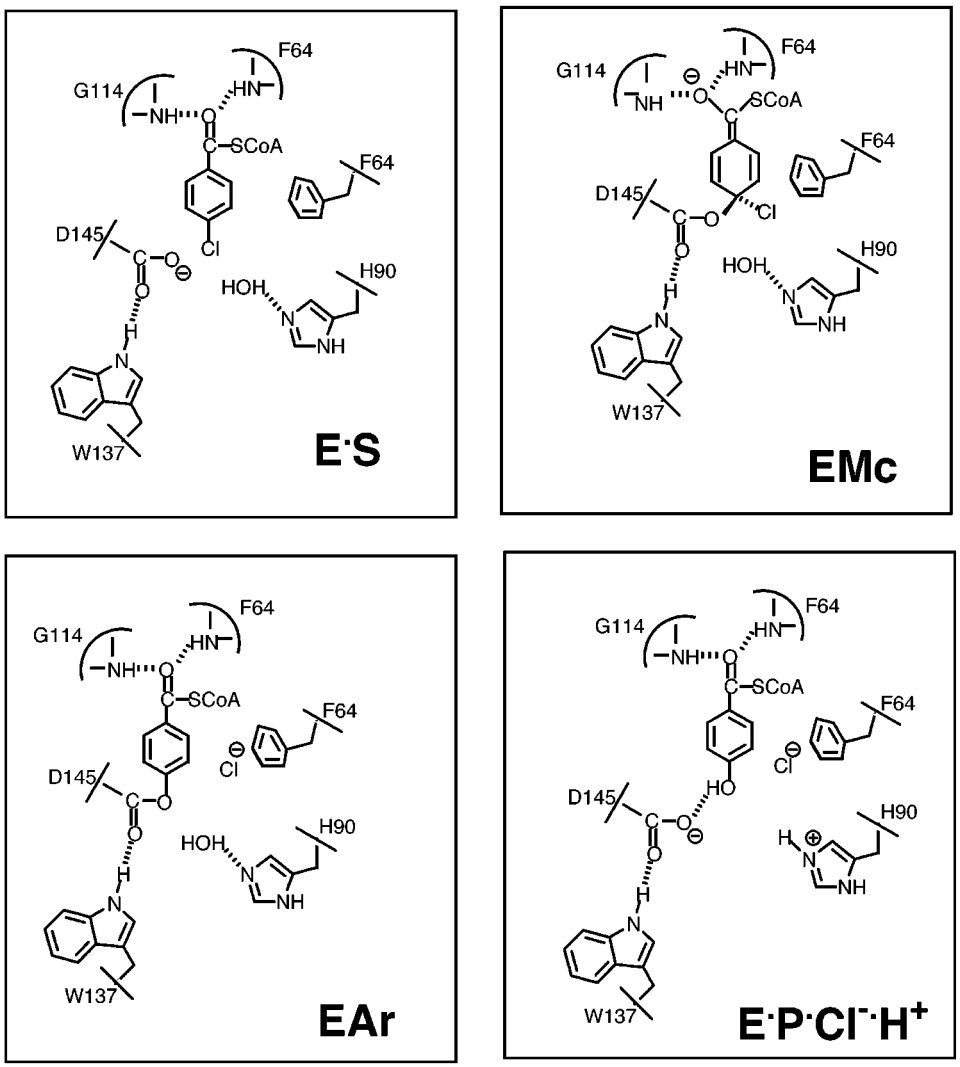

FIGURE 1: Steps of 4-CBA-CoA dehalogenase catalysis. The catalytic residues functioning in the enzyme−substrate (E·S), the Meisenheimer intermediate (EMc), the arylated enzyme intermediate (EAr), and the enzyme−product complex (E·P·Cl^-·H^+) are shown.

Scheme 1: Three-Step 4-CBA Degradation Pathway Found in Certain Soil-Dwelling Bacteria

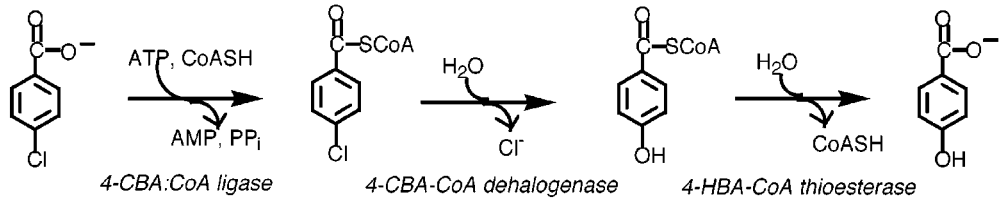

H-bonds to the benzoyl C═O group at the opposite end of the 4-HBA-CoA ligand, thereby connecting the two subsites on the enzyme. Because the 4-HBA-CoA ligand bends back on itself, adenosine N(7) and the pantetheine NH group can H-bond, as can the α-phosphate and the pantetheine C(OH) group. This study was carried out to determine the Gibbs free energies derived from these interactions in the enzyme−substrate complex and in the enzyme−transition state complex formed in the rate-limiting step.

EXPERIMENTAL PROCEDURES

General. Coenzyme A (CoA), 1,N^6-etheno-CoA (ϵ-CoA), 3′-dephospho-CoA, adenosine 3′,5′-diphosphate (3′,5′-ADP), adenosine 5′-monophosphate (5′-AMP), adenosine 5′-diphos-

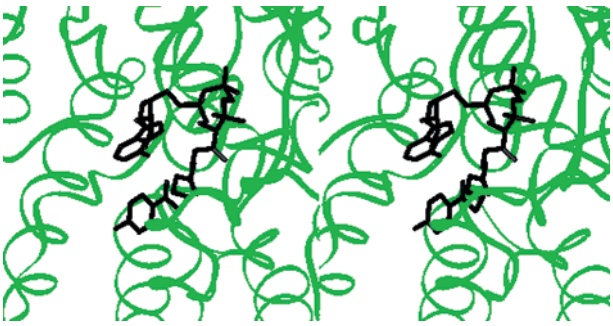

FIGURE 2: Stereodiagram of the 4-CBA-CoA dehalogenase active site with 4-HBA-3′-dephospho-CoA bound. The figure was generated using the X-ray crystallographic coordinates (*15*) using the molecular modeling program InsightII.

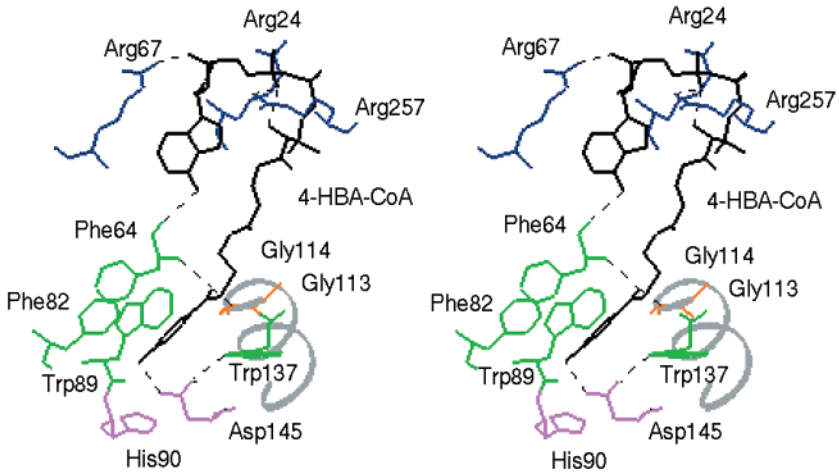

FIGURE 3: Stereodiagram of the 4-CBA-CoA dehalogenase active site with 4-HBA-3′-dephospho-CoA bound. The figure was generated using the X-ray crystallographic coordinates (*15*) using the molecular modeling program InsightII.

Chart 1

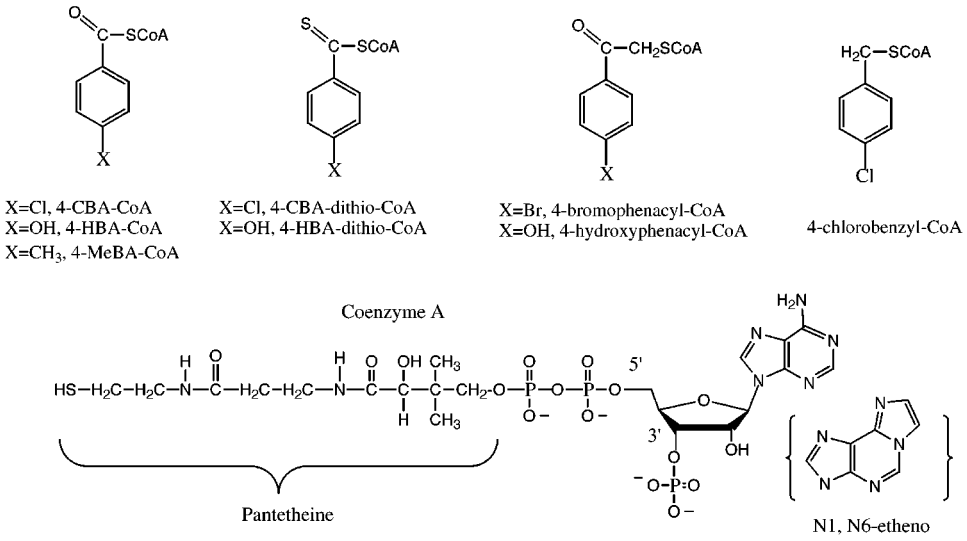

phate (ADP or 5′-ADP), adenosine 5′-triphosphate (ATP), nucleotide pyrophosphatase, bovine liver crotonase, and buffers were purchased from Sigma Chemical Co. All other chemicals were purchased from Aldrich. Dehalogenase concentrations were determined by using the Bradford method (*16*) or by measuring the UV absorbance of protein solutions at 280 nm (ϵ = 40 090 M^{-1} cm^{-1}). Enzyme spectrophotometric assays were carried out using Beckman DU640 or 7400 UV−vis spectrophotometers as previously described (*8*, *9*). ^{1}H NMR and ^{31}P NMR spectra were measured with a Bruker Advance 500 MHz or Bruker AC 250 MHz NMR spectrometer using D_2O as a solvent and a probe temperature of 24−26 °C. The chemical shift data are reported with respect to the external reference (trimethylsilyl)propanesulfonic acid for ^{1}H NMR and the internal reference phosphoric acid for ^{31}P NMR.

Preparation of Mutant Dehalogenases. R24K, R24L, R67K, R67L, R257K, R257L, G113A, F64P, and F64A dehalogenases were prepared using the standard "overlapping" PCR method (*17*). The cloned pT 7.5 plasmids were purified using the QIA prep spin plasmid kit and then used to transform *Escherichia coli* BL21(DE3) cells from Novagen. The overexpressed mutant enzymes were purified using the same procedure that was used for purification of wild-type dehalogenase (*11*). DNA sequences were verified by nucleotide sequencing carried out at the Center for Agricultural Biotechnology, University of Maryland (College Park, MD). The G114A and G114P dehalogenases were prepared as previously described (*13*).

Preparation of Dehalogenase Substrate and Product Analogues (Chart 1). The compounds 4-CBA-CoA, 4-MeBA-CoA, 4-HBA-CoA, 4-CBA-dithio-CoA, and 4-HBA-dithio-CoA were prepared as previously described (*9*, *12*, *27*). The compounds 4-CBA-3′-dephospho-CoA, 4-CBA-ϵ-CoA, 4-CBA-pantetheine, 4-MeBA-3′-dephospho-CoA, and 4-bromobenzyl-CoA were prepared from the commercially available acyl chloride precursors 4-chlorobezoyl chloride, 4-methylbenzoyl chloride, and 4-bromobezoyl bromide by direct reaction with the CoA or CoA analogue as described in ref *9*. 4-Bromophenylacetyl-CoA was prepared from 4-bromophenylacetyl bromide (synthesized from 4-bromophenone as reported in ref *20*) and CoA according to the procedures reported in ref *9*. The compounds 4-HBA-3′-dephospho-CoA, 4-HBA-pantetheine, and 4-hydroxyphenylacetyl-CoA were prepared from 4-hydroxybenzoic acid (Aldrich) and 4-hydrozylphenacyl bromide (synthesized from

4-hydroxyphenone as reported in ref *20*) by converting them to the anhydride derivative via reaction with ethyl chloroformate followed by reaction with the CoA or CoA derivative as described in ref *19*. 4-CBA-pantetheine phosphate was prepared from 4-CBA-CoA (10 μmol) by treatment with 5 units of nucleotide pyrophosphatase in 50 mM K^+Hepes buffer (20 mM $MgCl_2$, pH 7.0) at 37 °C for 10 h. The ^{1}H NMR and ^{31}P NMR spectral data of the compounds mentioned above are reported in the Supporting Information.

Steady State Kinetic Analysis. The steady state kinetic catalytic constants V_{max} and K_m and the competitive inhibition constant K_i were measured for wild-type (0.02 μM), R24K (0.02 μM), R24L (0.05 μM), R67K (0.05 μM), R257K (0.02 μM), R257L (0.1 μM) G113A (1.0 μM), F64P (1.0 μM), and F64A (0.03 μM) dehalogenase. The initial velocity of the catalyzed reaction was measured using the spectrophotometric assay described in ref *9*. Reactions were carried out in 50 mM K^+Hepes (pH 7.5, 25 °C) containing varying concentrations of 4-CBA-CoA ($^1/_2$−10-fold times K_m) with or without inhibitor. Inhibitor concentrations ranged between 1.5- and 4-fold times K_i. For all measurements, the initial velocity data were analyzed using eqs 1 and 2 and the computer programs of Cleland (*24*).

$$V = (V_{max}[S])/([A] + K_m) \quad (1)$$

$$V = (V_{max}[S])/[K_m(1 + [I]/K_i) + [A]] \quad (2)$$

where V is the initial velocity, V_{max} is the maximum velocity, [S] is the substrate concentration, K_m is the Michaelis constant, [I] is the inhibitor concentration, and K_i is the the inhibition constant. The k_{cat} was calculated from V_{max}/[E], where [E] is the total enzyme concentration.

The initial velocities of the dehalogenase (7.5 μM)-catalyzed reactions of 4-CBA-pantetheine phosphate and 4-CBA-pantetheine (500 μM) were measured in the presence and absence of 3′,5′-ADP (0.5−10.0 μM) or 5′-ADP (0.5−7.5 μM).

UV−Visible Absorption Difference Spectra of Enzyme−Ligand Complexes. UV−visible absorption difference spectra were measured as described in ref *13*. Reference spectra were measured using 1 mL quartz tandem cells containing 0.5 mL of enzyme solution in one compartment and 0.5 mL of a 4-HBA-CoA or 4-MeBA-CoA (or analogues) solution in the other. All solutions were buffered with 50 mM K^+Hepes (pH 7.5, 25 °C). The reference absorbance spectrum was recorded and subtracted from the spectrum of the mixed solutions to give the difference spectra of the enzyme−ligand complex. The apparent dissociation constants (K_d) of the enzyme−4-MeBA-CoA and enzyme−4-HBA-CoA complexes were measured by spectral titration. The absorbance due to the enzyme−ligand complex, determined from the difference spectrum, was measured as a function of ligand concentration at a fixed enzyme concentration. The 4-MeBA-CoA titrations were monitored at a λ_{max} of 302−308 nm, while the 4-HBA-CoA titrations were monitored at 373 nm (for R24L and R24K, R67K, R257L and R257K, and F64A mutants) or 318 nm (for the G113A mutant). The titration data were fitted to eq 3 as previously described (*25*).

$$\Delta A = (\Delta A_{max}/[E])[K_d + [E] + [S] - \sqrt{(K_d + [E] + [S])^2 - 4[E][S]}]/2 \quad (3)$$

In eq 3, ΔA_{max} is the the total change in absorbance, ΔA is the observed change in absorbance, [E] is the the total enzyme concentration, [S] is the ligand concentration, and K_d is the dissociation constant.

Calculation of $\Delta\Delta G_{ES}$ and $\Delta\Delta G^{\ddagger}$. Values for $\Delta\Delta G_{ES}$ (binding energy for the enzyme−substrate complex) and $\Delta\Delta G^{\ddagger}$ (binding energy for the rate-limiting transition state) were calculated from eqs 4 and 5 (*26*), where R is the gas constant (1.987 cal mol^{-1} K^{-1}) and T is temperature in kelvin (298 K).

$$\Delta\Delta G_{ES} = -RT \ln(K_d^{\text{obs,without group present}}/K_d^{\text{obs,with group present}}) \quad (4)$$

$$\Delta\Delta G^{\ddagger} = -RT \ln[(k_{cat}/K_m)^{\text{obs,without group present}}/(k_{cat}/K_m)^{\text{obs,with group present}}] \quad (5)$$

In eq 4, $K_d^{\text{obs,without group present}}$ and $K_d^{\text{obs,with group present}}$ represent the constants for dissociation of the ligand from the enzyme in the absence of the functional group (removed by either modification of the ligand structure or mutation of the interacting residue) and in the presence of the functional group, respectively. The K_i values obtained for the competitive inhibitors are treated as dissociation constants. The K_m values are considered as an approximation of K_d (when chemical steps are rate-limiting, $K_m = K_d$). For 4-CBA-CoA, the K_d calculated from the ratio of k_{off} (28 s^{-1}) to k_{on} (7 μM^{-1} s^{-1}) is 4 μM (W. Zhang and D. Dunaway-Mariano, unpublished data) which is comparable to the reported K_m of 3.7 μM (*13*). Thus, the assumption that $K_m = K_d$ is valid for the natural substrate with the wild-type enzyme. For substrate analogues and dehalogenase mutants in which catalysis is slowed, the assumption should surely hold.

In eq 5, $(k_{cat}/K_m)^{\text{obs,without group present}}$ and $(k_{cat}/K_m)^{\text{obs,with group present}}$ represent the k_{cat}/K_m values measured for reactions taking place in substrates and/or enzymes missing the functional group (by either modification of the ligand structure or mutation of the interacting residue) and possessing the functional group, respectively.

RESULTS AND DISCUSSION

Kinetic and Thermodynamic Constants Measured To Evaluate Binding Interactions between the Enzyme and the Substrate Coenzyme A Moiety

Enzyme Mutants. The enzyme residues positioned for ion pairing with the phosphoryl groups of the substrate CoA moiety are Arg24, Arg67, and Arg257. These residues were replaced with Lys to conserve the positive charge, and with Leu to remove the charge. The mutant enzymes were evaluated for their ability to bind the substrate analogue 4-MeBA-CoA and the product ligand 4-HBA-CoA, as well as the CoA unit of these ligands. The binding constants of these ligands were measured by spectral titration and/or competitive inhibition.[3] The steady state k_{cat} and K_m values

[3] The dissociation constants (K_d) measured from UV−differential titration experiments are typically 3−6-fold smaller than the K_i values measured from inhibition experiments. The reason for this discrepancy is not known. In the case of the titration experiment, the high enzyme concentration and the preincubation of the enzyme with ligand may contribute to the differences that are seen.

Table 1: Kinetic Constants (k_{cat} and K_m) for Wild-Type and Mutant 4-CBA-CoA Dehalogenase Catalysis and Dissociation Constants (K_d) and/or Inhibition Constants (K_i)[3] for 4-MeBA-CoA, 4-HBA-CoA, and CoA with Wild-Type and Mutant 4-CBA-CoA Dehalogenase (Measured at pH 7.5 and 25 °C in 50 mM K^+Hepes Buffer)

	4-CBA-CoA		4-MeBA-CoA	4-HBA-CoA	CoA
enzyme	k_{cat} (s^{-1})	K_m (μM)	K_i or K_d (μM)	K_i or K_d (μM)[3]	K_i (μM)
wild-type	0.60 ± 0.01	3.7 ± 0.3	4.2 ± 0.5[b] 0.5 ± 0.1[a]	2.5 ± 0.1[b] 0.6 ± 0.2[a]	140 ± 10[b]
R24L	0.33 ± 0.04	41 ± 7	46 ± 3[b]	16.5 ± 1.0[b] 8.1 ± 0.6[a]	660 ± 70[b]
R24K	0.95 ± 0.05	21 ± 2	11 ± 1[b] 9 ± 2[a]	2.4 ± 0.3[b] 0.5 ± 0.2[a]	250 ± 30[b]
R67K	0.38 ± 0.01	6.9 ± 0.7	51 ± 5[b] 13 ± 1[a]	6.2 ± 0.2[b] 2.4 ± 0.2[a]	520 ± 70[b]
R257L	0.14 ± 0.01	70 ± 9	72 ± 6[b]	19 ± 3[b] 20 ± 1[a]	2400 ± 300[b]
R257K	0.55 ± 0.01	5.8 ± 0.5	3.1 ± 0.3[b] 3.5 ± 0.9[a]	1.7 ± 0.3[b] 0.22 ± 0.06[a]	90 ± 10[b]

[a] Dissociation constants (K_d) measured from UV−differential titration experiments. [b] Inhibition constants (K_i) measured from inhibition experiments.

Table 2: Kinetic Constants and/or Inhibition Constants Measured for 4-CBA-CoA Structural Analogues as Substrates or as Competitive Inhibitors of Wild-Type 4-CBA-CoA Dehalogenase

inhibitor/substrate	k_{cat} (s^{-1})	K_m (μM)	K_i (μM)
4-CBA-CoA	0.60 ± 0.01	3.7 ± 0.3	
4-CBA-3′-dephospho-CoA	0.45 ± 0.01	20 ± 2	
4-MeBA-3′-dephospho-CoA			22 ± 2
4-CBA-ϵCoA	0.007 ± 0.0005	310 ± 30	
4-CBA-pantethiene phosphate	0.051 ± 0.003	440 ± 40	
4-CBA-pantethiene phosphate/2.5 mM 3′,5′-ADP	0.13 ± 0.01	260 ± 20	
4-CBA-pantethiene	∼0.001	>2000	
4-CBA-pantethiene/1 mM 5′-ADP	0.056 ± 0.005	70 ± 20	
ATP, 5′-AMP, 3′-AMP, 3′,5′-ADP, adenosine, PP_i			>5000
5′-ADP			4200 ± 400
CoA			140 ± 20
3′-dephospho-CoA			770 ± 70
4-CBA			21000 ± 1000

were measured to evaluate the ability of mutant enzymes to bind and turn over substrate at low concentrations (k_{cat}/K_m; E + S → E + P) and at saturating concentrations (k_{cat}; ES → E + P). The kinetic and thermodynamic constants obtained for the mutants are listed in Table 1.

The CoA binds to wild-type dehalogenase with moderate affinity (K_i = 140 μM). The Arg24 is aligned for interaction with the β-P of the CoA pyrophosphoryl group. Lys substitution at this position reduces the CoA binding affinity 2-fold, and Leu replacement reduces it 5-fold. Reductions are also observed in the binding affinities of 4-MeBA-CoA (Leu, 10-fold; Lys, 2.5-fold) and 4-HBA-CoA (Leu, 7-fold). The Arg24 mutations do not strongly inhibit catalytic turnover (minimal change in k_{cat}), but their impact on substrate binding is reflected in reduced k_{cat}/K_m values (Leu, 11-fold; Lys, 4-fold).

Arg67 is aligned for interaction with the 3′-phosphoryl group of the substrate CoA moiety. Unfortunately, the R67L mutant was expressed as an inclusion body and, thus, was not characterized. The R67K mutant binds CoA 4-fold less tightly than does the wild-type enzyme. Comparable reductions are observed in the binding affinities of 4-MeBA-CoA and 4-HBA-CoA, and reductions (3-fold) were observed in k_{cat}/K_m.

Arg257 is aligned for interaction with the β-P of the CoA pyrophosphoryl group. Lys substitution at this position does not reduce the CoA binding affinity; however, Leu substitution reduces it 17-fold. A similar trend is seen in the binding of 4-MeBA-CoA and 4-HBA-CoA. Catalytic function is almost fully retained in the R257K mutant, but it is significantly reduced in the R257L mutant (4-fold reduction in k_{cat} and 81-fold reduction in k_{cat}/K_m).

Table 3: Kinetic Constants (k_{cat} and K_m) for Wild-Type and Mutant 4-CBA-CoA Dehalogenase Catalysis and Dissociation Constants (K_d) and/or Inhibition Constants (K_i)[3] for 4-MeBA-CoA, 4-HBA-CoA, and CoA with Wild-Type and Mutant 4-CBA-CoA Dehalogenase (Measured at pH 7.5 and 25 °C in 50 mM K^+Hepes Buffer)

	4-CBA-CoA		4-MeBA-CoA	4-HBA-CoA
enzyme	k_{cat} (s^{-1})	K_m (μM)	K_i or K_d (μM)	K_i or K_d (μM)
wild-type	0.60 ± 0.01	3.7 ± 0.3	4.2 ± 0.5[b] 0.5 ± 0.1[a]	2.5 ± 0.1[b] 0.6 ± 0.2[a]
G113A	0.005 ± 0.001	14.3 ± 0.3	44 ± 6[b]	40 ± 4[b] 8.5 ± 0.9[a]
G114A	0.002	110 ± 10	−	50−100[b]
F64P	$<10^{-5}$	−	−	
F64A	0.03 ± 0.002	5.2 ± 0.4	0.6 ± 0.2[a]	1.4 ± 0.1[a]

[a] Dissociation constants (K_d) measured from UV−differential titration experiments. [b] Inhibition constants (K_i) measured from inhibition experiments.

Substrate Analogues. The 3′-dephospho-CoA and 4-MeBA-3′-dephospho-CoA were used in ligand binding studies to probe the interaction between Arg67 and the 3′-P of the substrate CoA moiety. The K_i values (Table 2) of these analogues are 5-fold larger than those of CoA and 4-MeBA-CoA (Table 3). 4-CBA-3′-dephospho-CoA undergoes catalysis as fast as 4-CBA-CoA under saturating conditions but 7-fold slower under nonsaturating conditions.

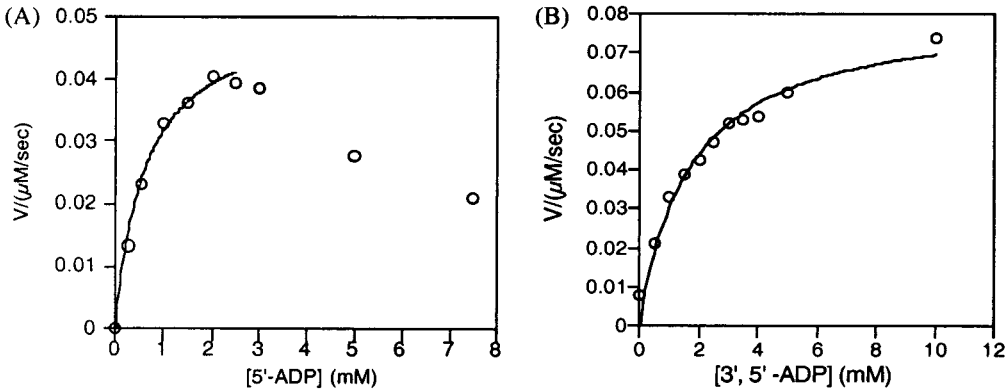

FIGURE 4: (A) Curve of the reaction rate (4-CBA-pantetheine with 4-CBA-CoA dehalogenase) vs the concentration of 5′-ADP. (B) Curve of reaction rate (4-CBA-pantetheine phosphate with 4-CBA-CoA dehalogenase) vs the concentration of 3′,5′-ADP added to the reaction solution.

4-CBA-pantetheine and 4-CBA-pantetheine phosphate were used to probe the contribution of the CoA nucleotide moiety to substrate binding and catalysis. First, the analogues were tested as substrates for the dehalogenase using the spectrophotometric assay in which the appearance of the 4-hydroxybenzoylpantetheine product is monitored by the increased absorbance at 310 nm. For both reactions, a noticeable lag in product formation preceded the attainment of the steady state rate. For example, the reaction of 2.6 mM 4-CBA-pantetheine with 7.5 μM dehalogenase showed no detectable product formation during the first 250 s of the reaction. After a lag period of ~600 s, slow product formation was observed, the rate of which eventually increased to a steady state rate of 4.5×10^{-3} s^{-1}. Inclusion of 1.0 mM 5′-ADP in the reaction eliminated the delay in the attainment of the steady state and allowed the measurement of k_{cat} (5.6×10^{-2} s^{-1}) and K_m (170 μM).

The initial velocity of the reaction of 4-CBA-pantethiene (500 μM) catalyzed by dehalogenase (7.5 μM) was measured as a function of 5′-ADP concentration. The results are plotted in Figure 4A. The plot reflects nucleotide activation at 5′-ADP concentrations of <2 mM. The apparent K_m for activation is ~0.6 mM. Higher concentrations of 5′-ADP resulted in reduced initial velocities. The origin of this inhibition was not examined.

The k_{cat} measured for 4-CBA-pantetheine phosphate is 5.0×10^{-2} s^{-1} (12-fold lower than that of 4-CBA-CoA), and the K_m is 440 μM (100-fold larger than that of 4-CBA-CoA) (Table 2). The k_{cat} of the reaction was increased to 0.13 s^{-1} and the K_m lowered to 260 μM when 2.5 mM 3′,5′-ADP was present in the reaction solution. The dependence of the initial velocity of the reaction on 3′,5′-ADP concentration was measured at fixed enzyme (1.0 μM) and 4-CBA-pantetheine phosphate (100 μM) concentrations (Figure 4B). The data, defining a hyperbolic curve, were used to obtain an apparent K_m for activation of 1.7 mM. These results indicate that synergistic binding occurs between 4-CBA-pantethiene and 5′-ADP and between 4-CBA-pantethiene phosphate and 3′,5′-ADP.

The ligands 3′-AMP, 5′-ADP, ATP, 5′-AMP, adenosine, and PP_i were tested as competitive inhibitors versus 4-CBA-CoA. No inhibition was observed at inhibitor concentrations up to 5 mM. 5′-ADP, on the other hand, was found to be a competitive inhibitor having a K_i of 4.0 mM (Table 2).

For the purpose of evaluating the contribution of the hydrogen bond between the AdeC(6)NH_2 and backbone carbonyl group of Phe64 (Figure 2) to ligand binding and catalysis, the kinetic constants of 4-CBA-ϵ-CoA, a substrate analogue having an ethylene bridge between N^1 and N^6 of the adenosine portion of CoA (Chart 1), were measured. On the basis of the observed k_{cat} of 7×10^{-3} s^{-1} and k_{cat}/K_m of 2.2×10^{-5} μM^{-1} s^{-1}, it is evident that the C(6)NH_2 group is essential to efficient catalysis, although it is not known what singular contribution removal of the H-bond interaction makes. The introduction of unfavorable steric interaction associated with the ethylene bridge may also contribute to impaired binding and catalysis.

Kinetic and Thermodynamic Constants Measured To Evaluate Binding Interactions between the Enzyme and the Substrate Benzoyl C═O Group

Enzyme Mutants. The substrate benzoyl C═O group is positioned to engage in H-bonding with the amide backbone NHs of Gly114 and Phe64. To evaluate the contribution of these H-bonds to substrate binding and catalysis, we examined the catalytic properties of F64P and G114A (G114P proved to be insoluble) dehalogenase mutants. Catalysis in F64P is severely impaired. In contrast, the F64A mutant was found to be only 30-fold less active (k_{cat} and K_m reported in Table 3) than wild-type dehalogenase, and the binding affinities of the 4-MeBA-CoA and 4-HBA-CoA ligands are unchanged. The electropositive edge of the Phe64 ring may interact favorably with the displaced halide (Figure 3) in the dehalogenase active site, thus accounting for the 30-fold reduction in the extent of catalysis observed for the F64A mutant.[4] In contrast, the majority of the 10^4-fold decrease in k_{cat} observed with the F64P mutant is attributed to the loss of H-bond interaction with the benzoyl C═O group. However, in the absence of an X-ray structure of the mutant enzyme, we cannot rule out the possibility that impaired catalysis is the result of a change in enzyme conformation.

Catalysis in the G114A and G113A dehalogenases is strongly inhibited as are the binding reactions of 4-MeBA-CoA and 4-HBA-CoA (Table 3). While the G114 backbone amide NH is still available for H-bonding in these two mutants, the added steric bulk of the Ala side chain at position 113 or 114 is apparently sufficient to offset the alignment of the donor−acceptor pair.

[4] Previous studies (*1*, *2*) have suggested that the benzene ring edge in the phenylalanine residue interacts favorably with negatively charged atoms.

Table 4: Kinetic and Inhibition Constants Measured for 4-CBA-CoA Analogues (See Chart 1 for Structures) as Substrates or as Competitive Inhibitors of Wild-Type 4-CBA-CoA Dehalogenase

inhibitor/substrate	k_{cat} (s^{-1})	K_m (μM)	K_i (μM)
4-chlorobenzyl-CoA	–	–	55 ± 6
4-CBA-dithio-CoA	0.003 ± 0.0002	33 ± 4	–
4-HBA-dithio-CoA	–	–	69 ± 7
4-bromophenacyl-CoA	0.03 ± 0.004	24 ± 3	–

Substrate Analogues. 4-Chlorobenzyl-CoA (Chart 1), an analogue of 4-CBA-CoA in which the benzoyl C═O group is replaced with a CH_2 group (and is therefore not available for H-bonding with Gly114 and Phe64), is not a substrate. The K_i of this analogue is 55 μM (see Table 4), ca. 15-fold larger than the K_i measured for the inert substrate analogue 4-MeBA-CoA.

The k_{cat} of 4-CBA-dithio-CoA, in which the benzoyl C═O group is replaced with sulfur, is 200-fold smaller (3.2×10^{-3} vs 0.6 s^{-1}) than that of 4-CBA-CoA, while the k_{cat}/K_m value is decreased 1760-fold (Table 4). 4-HBA-dithio-CoA binds 28-fold less tightly than does 4-HBA-CoA. Raman difference spectroscopic studies of 4-HBA-dithio-CoA complexed to wild-type dehalogenase have shown that the C═S group does not transmit the electron pulling forces of the Gly114 and Phe64 backbone amide NHs. This finding and decreased binding affinity are consistent with the reduced H-bonding capacity of the C═S group (*27*).

The keto analogue, 4-bromophenacyl-CoA, in which a methylene group bridges the benzoyl C═O group and the CoA sulfur displays a 20-fold reduction in k_{cat} and a 128-fold decrease in the k_{cat}/K_m compared to those of 4-bromobenzoyl-CoA (*9*) (Table 4).

Differential Use of Binding Energy To Stabilize the Substrate versus Transition State Enzyme Complexes

The kinetic data reported in Tables 1−4 were used to calculate $\Delta\Delta G_{ES}$, the contribution of a specific group on the substrate ligand to stabilization of the ES complex, and $\Delta\Delta G^{\ddagger}$, the contribution of a specific group on the substrate to the stabilization of the rate-limiting transition state complex (Table 5). The binding energies contributed by the CoA unit of the 4-CBA-CoA ligand in the ES complex ($\Delta\Delta G_{ES}$) and in the transition state ($\Delta\Delta G^{\ddagger}$) suggest that the CoA unit plays critical roles in securing the substrate into the active site and in reducing the energy barrier to turnover. In particular, the 3′-P,5′-ADP region of the CoA contributes 7.5 kcal/mol to dehalogenase transition state stabilization, 4.4 kcal/mol to stabilization of the ES complex, and, thus, 3.1 kcal/mol toward catalysis. Differential binding to the CoA moiety of acyl-CoA thioesters in catalysis by other enzymes has been noted in the literature. For example, Anderson and co-workers observed that 3′,5′-ADP activates crotonase-catalyzed hydration of 4-crotonylpantetheine (*28*, *29*). Jencks and co-workers found that in 3-oxoacid CoA transferase catalysis, the nucleotide domain of CoA contributes 8.9 kcal/mol toward stabilization of the transition state and only 2.2 kcal/mol toward stabilization of the ES complex (*30*, *31*). Similarly, in acyl-CoA dehydrogenase catalysis, the 3′,5′-ADP unit contributes an estimated 4.1 kcal/mol to transition state stabilization and only 1.6 kcal/mol to ES complex stabilization (*32*). Thus, the use of binding energy derived from interaction with the large CoA appendage to secure the substrate in the active site and drive catalysis may be commonplace among acyl-CoA-dependent enzymes.

Table 5: Binding Energies Derived from Noncovalent Interactions between Active Site Residues and Specific Regions of the 4-CBA-CoA Substrate in the Enzyme−Substrate Complex ($\Delta\Delta G_{ES}$) and Transition State Complex ($\Delta\Delta G^{\ddagger}$) (Values Defined within 10% Error)

region of substrate	$-\Delta\Delta G_{ES}$ (kcal/mol)	$-\Delta\Delta G^{\ddagger}$ (kcal/mol)
CoA	5.1[a]	–
3′,5′-ADP	3.0[b]	4.3[k]
3′-P,5′-ADP	4.4[c]	7.5[l]
3′-phosphate	1.0[d]	1.2[m]
5′-α-phosphate	1.7[e]	2.6[n]
5′-β-P	1.3[f]	1.8[o]
4-CBA-pantethiene phosphate	4.3[g]	–
4-CBA-pantethiene	3.2[h]	–
4-CBA	2.1[i]	–
benzoyl C═O	1.6[j]	4.9[p]

[a] Calculated from the K_i of 4-CBA and the K_m of 4-CBA-CoA with the wild-type enzyme. [b] Calculated from the K_m of 4-CBA-pantethiene phosphate and the K_m of 4-CBA-CoA with the wild-type enzyme. [c] Calculated from the K_m of 4-CBA-pantethiene and the K_m of 4-CBA-CoA with the wild-type enzyme. [d] Calculated from the average $\Delta\Delta G_{ES}$ of −1.0 kcal/mol from the K_m of 4-CBA-3′-dephospho-CoA and the K_m of 4-CBA-CoA with the wild-type enzyme, a $\Delta\Delta G_{ES}$ of −1.0 kcal/mol from the K_d of 4-MeBA-3′-dephospho-CoA and the K_d of 4-MeBA-CoA with the wild-type enzyme, and a $\Delta\Delta G_{ES}$ of −1.0 kcal/mol from the K_i of 3′-dephospho-CoA and the K_i of CoA with the wild-type enzyme. [e] Calculated from the average $\Delta\Delta G_{ES}$ of −1.7 kcal/mol from the K_m of 4-CBA-CoA with the R257L mutant and the wild-type enzyme, a $\Delta\Delta G_{ES}$ of −1.7 kcal/mol from the K_d of 4-MeBA-CoA with the R257L mutant and the wild-type enzyme, and a $\Delta\Delta G_{ES}$ of −1.7 kcal/mol from the K_i of CoA with the R257L mutant and the wild-type enzyme. [f] Calculated from the average $\Delta\Delta G_{ES}$ of −1.4 kcal/mol from the K_m of 4-CBA-CoA with the R24L mutant and the wild-type enzyme, a $\Delta\Delta G_{ES}$ of −1.4 kcal/mol from the K_d of 4-MeBA-CoA with the R24L mutant and the wild-type enzyme, and a $\Delta\Delta G_{ES}$ of −1.0 kcal/mol from the K_i of CoA with the R24L mutant and the wild-type enzyme. [g] Calculated from the K_i of 3′,5′-ADP and the K_m of 4-CBA-CoA with the wild-type enzyme. [h] Calculated from the K_i of 5′-ADP and the K_m of 4-CBA-3′-dephospho-CoA with the wild-type enzyme. [i] Calculated from the K_i of CoA and the K_m of 4-CBA-CoA with the wild-type enzyme. [j] Calculated from the K_i of 4-chlorobenzyl-CoA and the K_m of 4-CBA-CoA with the wild-type enzyme. [k] Calculated from the ratio of k_{cat}/K_m values derived from 4-CBA-pantethiene phosphate and 4-CBA-CoA with the wild-type enzyme. [l] Calculated from the ratio of k_{cat}/K_m values derived from 4-CBA-pantethiene and 4-CBA-CoA with the wild-type enzyme. [m] Calculated from the ratio of k_{cat}/K_m values derived from 4-CBA-3′-dephosphoCoA and 4-CBA-CoA with the wild-type enzyme. [n] Calculated from the ratio of k_{cat}/K_m values derived from 4-CBA-CoA with the R257L mutant and the wild-type enzyme. [o] Calculated from the ratio of k_{cat}/K_m values derived from 4-CBA-CoA with the R24L mutant and the wild-type enzyme. [p] Calculated from the ratio of k_{cat}/K_m values derived from the average $\Delta\Delta G^{\ddagger}$ of −4.4 kcal/mol from 4-CBA-dithio-CoA and 4-CBA-CoA with the wild-type enzyme and a $\Delta\Delta G^{\ddagger}$ of −5.4 kcal/mol from 4-CBA-CoA with the G114A mutant and the wild-type enzyme.

The substrate benzoyl C═O group also makes a significant, differential contribution to ES ($\Delta\Delta G_{ES} = -1.6$ kcal/mol) and transition state ($\Delta\Delta G^{\ddagger} = -4.9$ kcal/mol) stabilization in the dehalogenase. Thus, 3.3 kcal/mol of binding energy derived from interaction with the benzoyl C═O group is applied to catalysis.

The C═O group is positioned for H-bond formation with Gly114 and Phe64 backbone amide NHs. As seen within the dehalogenase−4-HBA-CoA complex, these H-bonds are 2.7 and 2.9 Å in length, respectively. The donor and acceptor

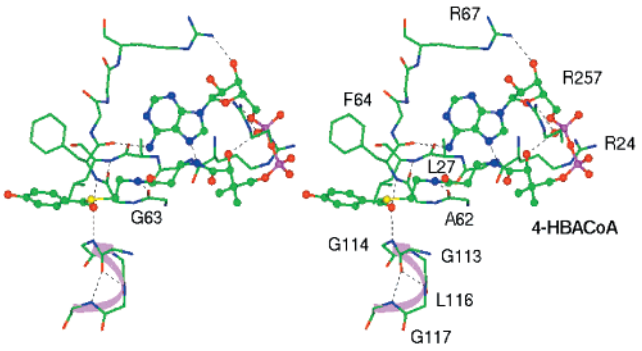

FIGURE 5: Stereoview of cooperative hydrogen bond networks in the active site of 4-CBA-CoA dehalogenase observed in the X-ray crystal structure of 4-CBA-CoA dehalogenase and the 4-HBA-CoA complex (*6*). The ligand 4-HBA-CoA is shown in a ball-and-stick representation, and the residues (24−27, 62−67, 113−117, and b257) are shown as sticks. The atom coloring scheme is as follows: C, green; O, red; N, blue; P, magenta; and S, yellow. The α-helix from G114 to G117 is represented by a pink ribbon. To provide a clear picture, only the backbones are shown for residues N25, A26, L27, A62, Y65, L66, and L116.

atoms appear to be optimally aligned for strong H-bond formation. We entertained the possibility that in the transition state leading to EMc formation these H-bonds might shorten, thus taking on the characteristics of the comparatively stronger low-barrier H-bond (LBHB) (*33*). To test this possibility, we measured the ^{1}H NMR spectra of the D145S and D145A dehalogenase−4-HBA-CoA complexes. Raman studies of these tight binding complexes have shown that, above pH 7, the benzoyl C(4)OH group of the bound 4-HBA-CoA ligand is fully ionized (*14*). The resulting enolate group of the bound quinoniod anion is analogous to that present in the EMc complex. Thus, our expectations were that if LBHBs formed as the ES complex proceeded to the EMc complex they would be present in the D145S and D145A dehalogenase−4-HBA-CoA complexes at pH 7.5. The ^{1}H NMR spectra (data not shown), measured with water suppression, were devoid of downfield resonances characteristic of the LBHB (*34*), thus indicating that LBHB formation does not contribute to dehalogenase catalysis.

How then might the two H-bonds to the C═O group in the ES complex gain strength in the transition state? One possibility is that as the charge density on the oxygen atom is increased, the resulting increase in the electrostatic interaction is amplified through the two H-bond networks seen to connect with the Gly114 and Phe64 backbone amide NH H-bonds. As shown in Figure 5, one of these H-bond networks includes (1) the H-bond between the Gly114 backbone amide NH group and the thioester carbonyl C═O group, (2) the bifurcated 1−3 and 1−4 H-bond between the Gly113 backbone C═O group and backbone amide groups of Leu116 and Gly117, (3) the H-bond between the Phe64 backbone amide NH group and thioester carbonyl C═O group and the Phe64 backbone C═O H-bond with the adenosine C(6)NH2 group, (4) the H-bond between the Gly63 backbone C═O group and the backbone amide NH group of Leu27, (5) the H-bond between the Ala62 backbone C═O group and the amide NH group of the *N*-acetylcysteamine group of CoA, and (6) the H-bond formed between adenosine N(7) and the pantetheine NH group. The second network consists of the H-bond between the α-phosphate and the pantetheine C(OH) group, the H-bond formed between Arg257 and the α-phosphate group of CoA, and the H-bond between Arg24 and the β-phosphate group of CoA.

Recently, Guo and Salahub reported the results of density function calculations which showed the large cooperative effect induced by the interaction of an anion with a peptide hydrogen bond network (*35*). These workers suggested that a cooperative H-bonding might be used by an enzyme to differentially stabilize a negatively charged transition state over the substrate. In addition, quantum mechanical calculations also indicated that helices having an α_N-type distortion at the N-terminus (which always involves residue at the N-terminus of the α-helix forming a bifurcated 1−4 and 1−5/1−3 hydrogen bond) may be particularly effective in charge stabilization.

In 4-CBA-CoA dehalogenase, the ligand benzoyl carbonyl group serves as an extension to connect the H-bonding network from two structural units, one α-helix segment (G114−G121) and one loop segment (A62−R67). As the reaction proceeds, the developing negative charge at the carbonyl oxygen of the thioester might be stabilized by the strong cooperative effect induced by the interactions with the C═O group. We hypothesize that to optimize this cooperative effect, the CoA ligand assumes an unusual highly bent structure[5] which allows the nucleotide moiety of CoA to participate in the H-bond network. This may also explain how the nucleotide domain of CoA can bring about the large increase in the rate of dehalogenase catalysis (Table 5). Indeed, a very similar cooperative hydrogen bond network can be identified in the X-ray crystal structure of 2-enoyl-CoA hydratase (crotonase) bound with acetoacetyl-CoA, in which the thioester carbonyl group is the connection for two local H-bond networks involving almost identical H-bonds seen in dehalogenase (*36*, *37*). Thus, we expect that the differential expression of binding energy at the ground state and the transition state via cooperative H-bonding could be a common strategy used in catalysis by enzymes in the 2-enoyl-CoA hydratase/isomerase superfamily (*38*, *39*).

[5] The H-bond formed between the pantetheine N″1 amide proton and adenosine N(7) is unique among all known bound CoA structures except for that observed in the crotonase-acetoacetyl-CoA structure. In all other known CoA binding proteins, this distance is at least 5.2 Å (*3*).

ACKNOWLEDGMENT

Debbie A. Miller and Claire Tseng at Harvard Medical School are gratefully acknowledged for their comments on the manuscript.

SUPPORTING INFORMATION AVAILABLE

Spectral properties of coenzyme A derivatives. This material is available free of charge via the Internet at http://pubs.acs.org.

REFERENCES

1. Burley, S. K., and Petsko, G. A. (1986) *FEBS Lett. 203*, 139−143.
2. Thomas, K. A., Smith, G. M., Thomas, T. B., and Feldmann, R. J. (1982) *Proc. Natl. Acad. Sci. U.S.A. 79*, 4843−4847.
3. Wu, W. J., Tonge, P. J., and Raleigh, D. P. (1998) *J. Am. Chem. Soc. 120*, 9988−9994.

4. Dunaway-Mariano, D., and Babbitt, P. C. (1994) *Biodegradation 5*, 259−276.
5. Harayama, S., Rekik, M., Wubbolts, M., Rose, K., Leppik, R. A., and Timmis, K. N. (1989) *J. Bacteriol. 171*, 5048−5055.
6. Liu, R. Q., Liang, P. H., Scholten, J., and Dunaway-Mariano, D. (1995) *J. Am. Chem. Soc. 117*, 5003−5004.
7. Crooks, G. P., Xu, L., Barkley, R. M., and Copley, S. D. (1995) *J. Am. Chem. Soc. 117*, 10791−10798.
8. Chang, K. H., Liang, P. H., Beck, W., Scholten, J. D., and Dunaway-Mariano, D. (1992) *Biochemistry 31*, 5605−5610.
9. Liang, P. H., Yang, G., and Dunaway-Mariano, D. (1993) *Biochemistry 32*, 12245−12250.
10. Yang, G., Liang, P. H., and Dunaway-Mariano, D. (1994) *Biochemistry 33*, 8527−8531.
11. Yang, G., Liu, R. Q., Taylor, K. L., Xiang, H., Price, J., and Dunaway-Mariano, D. (1996) *Biochemistry 35*, 10879−10885.
12. Taylor, K. L., Liu, R. Q., Liang, P. H., Price, J., Dunaway-Mariano, D., Tonge, P. J., Clarkson, J., and Carey, P. R. (1995) *Biochemistry 34*, 13881−13888.
13. Taylor, K. L., Xiang, H., Liu, R. Q., Yang, G., and Dunaway-Mariano, D. (1997) *Biochemistry 36*, 1349−1361.
14. Dong, J., Xiang, H., Luo, L., Dunaway-Mariano, D., and Carey, P. R. (1999) *Biochemistry 38*, 4198−4206.
15. Benning, M. M., Taylor, K. L., Liu, R.-Q., Yang, G., Xiang, H., Wesenberg, G., Dunaway-Mariano, D., and Holden, H. M. (1996) *Biochemistry 35*, 8103−8109.
16. Bradford, M. M. (1976) *Anal. Biochem. 72*, 248−254.
17. Erlich, H. A. (1992) *PCR Technology Principles and Applications for DNA Amplification*, W. H. Freeman and Co., New York.
18. Mieyal, J. J., Webster, L. T., and Siddigui, U. A. (1974) *J. Biol. Chem. 249*, 2633−2639.
19. Merkel, S. M., Eberhard, A. E., Gibson, J., and Harwood, C. S. (1989) *J. Bacteriol. 171*, 1−7.
20. King, L. C., and Ostrum, K. (1964) *J. Org. Chem. 29*, 3459−3464.
21. Taylor, K. L. (1996) Ph.D. Thesis, University of Maryland, College Park, MD.
22. Butler, J., Speilberg, S., and Schulman, J. (1976) *Anal. Biochem.*, 674−675.
23. Liang, P.-H. (1994) Ph.D. Thesis, University of Maryland, College Park, MD.
24. Cleland, W. W. (1979) *Methods Enzymol. 63*, 103−137.
25. Anderson, K. S., Sikorski, J. A., and Johnson, K. A. (1988) *Biochemistry 27*, 7395−7406.
26. Narlikar, G. J., and Herschlag, D. (1998) *Biochemistry 37*, 9902−9911.
27. Dong, J., Luo, L., Liang, P.-H., Dunaway-Mariano, D., and Carey, P. R. (2000) *J. Raman Spectrosc. 31*, 365−371.
28. Bahnson, B. J., and Anderson, V. E. (1989) *Biochemistry 28*, 4173−4181.
29. Bahnson, B. J., and Anderson, V. E. (1991) *Biochemistry 30*, 5894−5906.
30. Whitty, A., Fierke, C. A., and Jencks, W. P. (1995) *Biochemistry 34*, 11678−11689.
31. Fierke, C. A., and Jencks, W. P. (1986) *J. Biol. Chem. 261*, 7603−7606.
32. Srivastava, D. K., Kumar, N. R., and Peterson, K. L. (1995) *Biochemistry 34*, 4625−4632.
33. Cleland, W. W., Frey, P. A., and Gerlt, J. A. (1998) *J. Biol. Chem. 273*, 25529−25532.
34. Zhao, Q., Abeygunawardana, C., Talalay, P., and Mildvan, A. S. (1996) *Proc. Natl. Acad. Sci. U.S.A. 93*, 8220−8224.
35. Guo, H., and Salahub, D. R. (1998) *Angew. Chem., Int. Ed. 37*, 2985−2990.
36. Engel, C. K., Kiema, T. R., Hiltunen, J. K., and Wierenga, R. K. (1998) *J. Mol. Biol. 275*, 847−859.
37. Engel, C. K., Mathieu, M., Zeelen, J. P., Hiltunen, J. K., and Wierenga, R. K. (1996) *EMBO J. 15*, 5135−5145.
38. Xiang, H., Luo, L., Taylor, K. L., and Dunaway-Mariano, D. (1999) *Biochemistry 38*, 7638−7652.
39. Babbitt, P. C., and Gerlt, J. A. (1997) *J. Biol. Chem. 272*, 30591−30594.

BI011536F